Contribution from the Department of Chemistry,
University of Cincinnati, Cincinnati, Ohio 45221

Thin-Layer Spectroelectrochemical Studies of Cobalt and Copper Schiff Base Complexes

DAVID F. ROHRBACH, WILLIAM R. HEINEMAN,*[1] and EDWARD DEUTSCH*[1]

Received March 5, 1979

A series of 19 cobalt and copper Schiff base complexes has been studied in *N,N*-dimethylformamide by thin-layer electro- and spectroelectrochemistry employing a gold minigrid optically transparent thin-layer electrode. The cobalt complexes exhibit Nernstian reversibility for both Co(II)/Co(III) and Co(I)/Co(II) couples, even though many exhibit only quasi-reversible behavior when studied by conventional bulk solution cyclic voltammetry. For closely related cobalt complexes there is a qualitative correlation between $E^{\circ\prime}$ for cobalt(II) reduction and the energy of the metal-to-ligand charge-transfer band of the cobalt(I) complex. $E^{\circ\prime}$ for the Co(II)/Co(III) couple is relatively insensitive to the structure of the equatorial ligand. $E^{\circ\prime}$ for the Co(I)/Co(II) couple is markedly dependent upon the degree of unsaturation in the equatorial Schiff base, greater unsaturation stabilizing the cobalt(I) form. The copper complexes also show Nernstian reversibility for the Cu(I)/Cu(II) couple under thin-layer conditions. The copper(I) complexes are stabilized by ligand unsaturation to the same extent as are the cobalt(I) analogues. Reduction of Cu(II) complexes generally occurs more easily than reduction of the analogous Co(II) complexes. Values of $E^{\circ\prime}$ for the Cu(I)/Cu(II) and Co(I)/Co(II) couples, as ligand structures are varied, are linearly related to each other, implying that the effects of equatorial ligand structure variation on $E^{\circ\prime}$ values are coherent and therefore predictable from one system to the next. This work demonstrates the efficacy and utility of thin-layer spectroelectrochemical methodology in a nonaqueous inorganic redox system.

Introduction

A recurrent theme in bioinorganic chemistry[2-8] has been quantitative evaluation of the effect of variation in equatorial ligand structure on the redox potential of macrocyclic cobalt and copper complexes and on Schiff base complexes used as models for some of the biological macrocycles.[9-12] Several researchers have proposed that the redox potential of the central metal ion in macrocyclic and Schiff base complexes is directly related to many of the biologically relevant chemical characteristics of the entire complex, e.g., dioxygen binding ability[13,14] and nucleophilicity.[15] Thus, there has been, and continues to be,[16] a strong interest in determining thermodynamically meaningful redox potentials of copper and cobalt Schiff base complexes and in understanding the relationship(s) between these potentials and the detailed structure of the Schiff base ligand.

Early electrochemical investigations of Schiff base complexes of transition metal ions were conducted primarily via polarography. Calvin and Bailes[17] studied the polarographic reduction of bridged and nonbridged copper complexes in aqueous pyridine and found a correlation of $E_{1/2}$ for Cu(II) → Cu(I) with the thermodynamic stability of the solution complexes. Urwin and West,[18] in a polarographic study of nonbridged cobalt complexes in aqueous ethylene glycol, discovered that both metal and ligand are reduced in this protic environment.

More recent electrochemical studies of these complexes have included such techniques as cyclic voltammetry, controlled-potential electrolysis, and controlled-potential coulometry. Costa et al.[15,19-21] have conducted a wide-ranging polarographic and cyclic voltammetric study of cobalt Schiff base complexes, organometallic derivatives, and optically active complexes and their oxygen adducts. Holm and Patterson[22] have recently reported an extensive investigation into the effects of structural variation on the polarographic $E_{1/2}$ values for copper complexes of various types, including Schiff base complexes. This elegant study employed *N,N*-dimethylformamide (DMF) as solvent and by controlled-potential coulometry determined the number of electrons transferred in the reductions. Addison has investigated one-electron redox processes at binuclear copper centers[23] and the redox properties of pseudotetrahedral copper Schiff base complexes as models for copper proteins.[24]

Thin-layer spectroelectrochemistry has been increasingly applied to the study of redox systems[25-27] since its development in 1967.[28] The simultaneous recording of spectrophotometric and electrochemical data is an important feature of the electrochemical cell that employs an optically transparent thin-layer electrode (OTTLE). Cyclic voltammetry, controlled-potential coulometry, and spectroelectrochemistry (specifically the spectropotentiostatic technique[29]) employing the OTTLE allow the determination of thermodynamically meaningful redox potentials ($E^{\circ\prime}$), the number of electrons involved in the redox process (n), and the spectra of electrogenerated species. This report then describes the application of these new techniques to a study of structurally related cobalt and copper Schiff base complexes in DMF.[30] The overall aim of this work has been to correlate the electrochemical and spectral properties of the metal complexes with the electronic and steric characteristics of the variously substituted Schiff base ligands. In the process of achieving this aim we have also demonstrated the efficacy and utility of thin-layer spectroelectrochemical methodology in a nonaqueous inorganic redox system.

Nomenclature

Specific nomenclature and acronyms used in identifying ligands and complexes are given in Table I. In describing redox processes we have employed the standard formalism wherein the total electron change is ascribed to the metal center regardless of any participation by ligand-centered orbitals.

Experimental Section

Syntheses. Schiff base ligands were prepared by standard literature procedures and recrystallized from ethanol or methanol. The ligands $(sal)_2$(3,4-DAEB), $(sal)_2$(2,3-DAN), $(naph)_2$(3,4-DAEB), and $(naph)_2$(2,3-DAN) have not been reported previously. Cobalt complexes were prepared by a slight modification of the method of Halpern, Marzilli, and Marzilli.[31] The solid reaction products were washed with methanol and diethyl ether in a nitrogen-filled glovebox; after drying in vacuo the products were stored in the glovebox under nitrogen. Copper complexes were synthesized in a similar fashion, except that ethanol was used as the reaction solvent and an inert atmosphere was not employed. Ligands and complexes were characterized by visible–UV spectrophotometry in CH_2Cl_2 and DMF, as well as by infrared spectral analysis.[32] In addition, many ligands were characterized by melting point, mass spectral analysis, and ^1H NMR analysis.[32] The homogeneity of all metal complex preparations was confirmed by TLC analysis.[32] Table II lists parameters characterizing those ligands and metal complexes that have not been previously reported. Table III lists elemental analysis data for selected ligands and complexes; elemental analyses were performed by Galbraith Laboratories, Inc., Knoxville, Tenn.

Instrumentation. Visible–UV and near-infrared spectra were recorded on a Cary 14 spectrophotometer. The cell compartment of

0020-1669/79/1318-2536$01.00/0

Table I. Abbreviations for Metal Complexes of Schiff Base Ligands

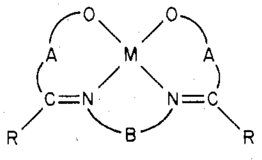

M = Co, Cu

R	A	B	abbrevn	ligand name
H	o-C_6H_4	$-CH_2CH_2-$	M[(sal)$_2$en]	bis(salicylaldehyde) ethylenediimine
H	o-C_6H_4	o-C_6H_4	M[(sal)$_2$DAB]	bis(salicylaldehyde) o-phenylenediimine
H	o-C_6H_4	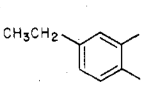	M[(sal)$_2$(3,4-DAEB)]	bis(salicylaldehyde) 3-ethyl-o-phenylenediimine
H	o-C_6H_4	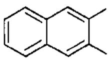	M[(sal)$_2$(2,3-DAN)]	bis(salicylaldehyde) 2,3-naphthalenediimine
CH_3	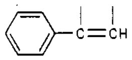	$-CH_2CH_2-$	M[(benac)$_2$en]	bis(benzoylacetone) ethylenediimine
H	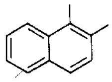	$-CH_2CH_2-$	M[(naph)$_2$en]	bis(2-hydroxy-1-naphthaldehyde) ethylenediimine
H	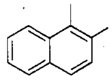	o-C_6H_4	M[(naph)$_2$DAB]	bis(2-hydroxy-1-naphthaldehyde) o-phenylenediimine
H	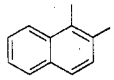	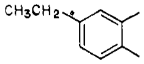	M[(naph)$_2$(3,4-DAEB)]	bis(2-hydroxy-1-naphthaldehyde) 3-ethyl-o-phenylenediimine
H	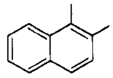	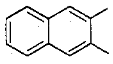	M[(naph)$_2$(2,3-DAN)]	bis(2-hydroxy-1-naphthaldehyde) 2,3-naphthalenediimine
CH_3	$CH_3\overset{\vert}{C}=\overset{\vert}{C}H$	$-CH_2CH_2-$	M[(acac)$_2$en]	bis(acetylacetone) ethylenediimine

Table II. Characterization of New Ligands and Metal Complexes

compd	mp, °C	electronic spectrum[a]	^{1}H NMR spectrum[b]
(sal)$_2$(3,4-DAEB)	98–102	480 sh, 365 sh, 334 (21 100)	1.2 t (3 H), 2.6 q (2 H), 7.0 m (10 H), 8.5 s (2 H), 12.2 s (2 H) (CCl_4)
(sal)$_2$(2,3-DAN)	195–196.5 dec	360 sh, 335 (28 300), 320 sh	7.5 m (13 H), 8.6 s (2 H), 11.1 bs (2 H) ($CDCl_3$)
(naph)$_2$(3,4-DAEB)	182–184	474 sh (12 300), 452 (14 500), 400 sh (20 100), 384 (20 700), 321 (19 600)	1.3 t (3 H), 2.8 q (2 H), 7.6 m (15 H), 8.95 s (2 H), 14.5 bs (2 H) ($CDCl_3$)
(naph)$_2$(2,3-DAN)	209–215 dec	474 (11 800), 450 (14 200), 386 (19 700), 322 (20 200)	7.4 m (20 H), 9.4 s (2 H) ($CDCl_3$)
Co[(sal)$_2$(3,4-DAEB)]	278–282 dec	670 sh, 570 sh (1800), 465 sh (9000), 388 (17 800), 380 sh (17 600), 330 sh (17 700)	
Co[(sal)$_2$(2,3-DAN)]·H_2O	>300	660 sh, 550 sh, 475 sh, 401 (22 600), 340 sh, 307 (26 700)	
Co[(naph)$_2$(3,4-DAEB)]	>300	695 sh, 470 sh (14 200), 445 (15 400), 401 (17 600), 382 sh (15 600), 322 sh (17 600)	
Co[(naph)$_2$(2,3-DAN)]	>300	580 sh, 500 sh, 435 sh (22 100), 413 (23 200), 342 sh (22 400)	
Cu[(sal)$_2$(3,4-DAEB)]	254–256 dec	560 (290), 422 (20 700), 400 (16 600), 346 (13 900), 304 (23 000)	
Cu[(sal)$_2$(3,4-DAN)]·H_2O	>300	584 sh (260), 445 sh, 423 (22 200), 352 sh (12 500), 332 sh, 320 (21 100), 306 (19 500)	
Cu[(naph)$_2$(3,4-DAEB)]	>300	608 sh, 487 sh (15 300), 462 sh (21 100), 426 (33 600), 360 sh (12 800), 344 sh (19 900), 332 (21 400)	
Cu[(naph)$_2$(2,3-DAN)]·H_2O	>300	620 sh (480), 470 sh (26 500), 434 (39 100), 360 sh (14 600), 332 (22 400)	

[a] λ, nm (ϵ); in DMF at ambient temperature. [b] Chemical shifts (δ) relative to Me_4Si and measured on a Varian T-60 NMR instrument.

this instrument was modified to accommodate electrical leads to a Lucite cell holder for spectroelectrochemistry with the OTTLE.[29] Electrochemistry was performed with a conventional operational amplifier potentiostat.[33] The working electrode was an OTTLE constructed from 100 or 500 wires/in. gold minigrid as previously described.[29,30] In one case, a mercury-coated gold OTTLE was used to extend the negative potential range.[34,35] A coiled platinum wire served as auxiliary electrode, and an aqueous saturated sodium chloride calomel electrode (NaSCE) of the H-cell type[35] was the reference electrode. The NaSCE was connected to the sample by a salt bridge consisting of a polyethylene tube with a Vycor plug and containing 0.5 M tetraethylammonium perchlorate (TEAP) in DMF. All potentials are expressed vs. this electrode and are uncorrected for junction potentials. OTTLE cells were calibrated for cell volume and optical thickness in one or both of two ways: electrochemically by coulometry on a standard solution of potassium ferricyanide[29] and spectrophotometrically with standard dichromate solution.[36] All results were recorded on a Houston Omnigraphic Model 2000 X-Y recorder

Table III. Elemental Analyses for Schiff Base Complexes

complex	% C calcd	% C found	% H calcd	% H found	% N calcd	% N found	% M calcd	% M found
$Co[(sal)_2en]$	59.09	59.09	4.34	4.40	8.61	8.56	18.12	18.00
$Co[(sal)_2DAB]$	64.35	64.69	3.78	3.93	7.50	7.41	15.79	16.05
$Co[(sal)_2(2,3\text{-}DAN)]\cdot H_2O$	65.31	65.35	4.11	4.32	6.35	6.21	13.35	13.68
$Co[(benac)_2en]$	65.18	65.37	5.48	5.48	6.91	6.91	14.54	14.62
$Co[(naph)_2en]$	67.77	67.94	4.27	4.30	6.59	6.98	13.85	13.01
$Co[(naph)_2(2,3\text{-}DAN)]$	73.42	73.18	3.86	3.84	5.35	5.31	11.26	10.45
$Cu[(sal)_2(2,3\text{-}DAN)]\cdot H_2O$	64.64	64.94	4.07	4.07	6.28	6.21	14.23	13.57
$Cu[(naph)_2(2,3\text{-}DAN)]\cdot H_2O$	70.38	69.86	4.06	3.98	5.13	5.34	11.64	11.73

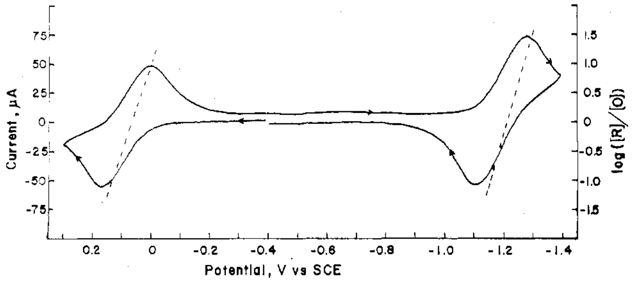

Figure 1. Left axis (—): thin-layer cyclic voltammogram of 2.0 mM $Co[(naph)_2en]$ in 0.5 M TEAP/DMF; scan rate 2 mV/s. Right axis (---): Nernstian plots of log ([R]/[O]) vs. E_{app} for Co(II)/Co(III) and Co(I)/Co(II) couples.

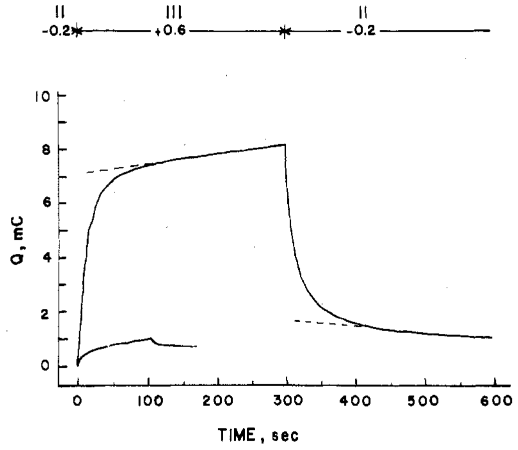

Figure 2. Thin-layer coulogram for 1.74 mM $Co[(sal)_2DAB]$ in 0.5 M TEAP/DMF, Co(II)/Co(III) couple. Bottom coulogram is for supporting electrolyte.

with time base or a Hewlett-Packard Model 7015A. A digital multimeter (United Systems Corp. Model 261C or Fluke Model 8000A) was used to monitor potentials.

Procedure. All experiments were conducted in DMF (Fisher Certified) made 0.5 M in polarographic grade TEAP (G. F. Smith and Eastman). Cyclic voltammetric experiments detected no significant difference between purified[37] and reagent grade DMF; most of the results reported herein were obtained with reagent grade DMF. Sample solutions were thoroughly deoxygenated by extended argon bubbling and then transferred to the electrochemical cell via Teflon tubing and argon pressure. The cell was positioned in the Cary 14 sample compartment (previously purged with argon) and a blanket of inert gas was maintained over the sample solution throughout the experiment. The sample compartment was sealed with clear polyethylene.

Results

Cobalt Complexes. Figure 1 shows the thin-layer cyclic voltammogram for $Co[(naph)_2en]$. A scan initiated in the positive direction at −0.4 V reveals an oxidation wave at +0.155 V. Upon reversal of the scan at +0.3 V, a reduction wave at +0.010 V is observed. By averaging the E_{p_a} and E_{p_c} values, we calculate an $E^{\circ\prime}$ value of +0.083 V; this couple has been[19] assigned to Co(II)/Co(III). The peak separation of 145 mV is due to *iR* drop inherent in the OTTLE cell and to the quasi-reversibility of this redox process (confirmed by bulk-solution cyclic voltammetry). Continuing the scan in the negative direction results in a reduction wave at −1.280 V. After scan reversal at −1.4 V, an oxidation wave is observed at −1.125 V. This couple with ΔE_p = 155 mV and $E^{\circ\prime}$ = −1.202 V has been assigned[19] to the Co(II)/Co(I) process. Multiple scans yielded nearly superimposable cyclic voltammograms, indicating the marked stability, and facile interconversion, of the three oxidation states of cobalt in these compounds.

Results of a typical thin-layer coulometry experiment are shown in Figure 2 for the $Co[(sal)_2DAB]$ $Co(II) \rightleftharpoons Co(III)$ process. The initial applied potential was −0.2 V. When the initial charging current decayed to a minimum, the potential was switched to +0.6 V and the charge vs. time results were recorded as Co(II) was oxidized to Co(III). The *Q–t* curve rapidly (ca. 3 min) leveled off, and at *t* = 5 min, the potential was stepped back to −0.2 V, resulting in reduction back to Co(II). A similar experiment was performed on the solvent/supporting electrolyte alone to determine the background contribution to the *Q–t* curve. Faraday's law in the form of eq 1 was then employed to determine *n*, the number of

$$Q_F = Q_T - Q_B = nFVC \qquad (1)$$

electrons transferred in the oxidation and reduction. The Faradaic charge, Q_F, is determined by subtracting the background charge, Q_B, from the total charge, Q_T, after extrapolating both curves to zero time. Knowledge of the volume of the OTTLE cell (see the Experimental Section), *V*, and the concentration of electroactive species, *C*, allows the calculation of *n*. For $Co[(sal)_2DAB]$ n = 1.01 ± 0.05 electrons for Co(II) → Co(III) and 0.97 ± 0.05 electrons for Co(III) → Co(II).

Application of the spectropotentiostatic method allows determination of $E^{\circ\prime}$, *n*, and spectra of fully oxidized and reduced species in one unified experiment. In this experiment, a series of potentials are applied to the OTTLE, and individual spectra are measured after equilibrium is attained at each potential as monitored by current decay to a small, essentially zero, value. Figure 3 shows such results for the oxidation of $Co[(naph)_2en]$. The absorbance changes at a given wavelength can be related to the concentration ratio of reduced to oxidized species by eq 2, where A_2 is the absorbance of the mixture of

$$[R]/[O] = (A_2 - A_3)/(A_1 - A_2) \qquad (2)$$

oxidized and reduced forms, A_1 is the absorbance of the totally reduced form, and A_3 is the absorbance of the totally oxidized form. The Nernst equation (3) indicates that a plot of E_{app}

$$E_{app} = E^{\circ\prime} - (0.059/n)\log([R]/[O]) \qquad (3)$$

vs. log ([R]/[O]) should be linear with a slope of 59/*n* mV and an intercept of $E^{\circ\prime}$, assuming Nernstian reversibility. Figure 1 shows two such plots for $Co[(naph)_2en]$. For the Co(II) oxidation $E^{\circ\prime}$ = +0.064 V and *n* = 0.92 electron (slope = 64.1 ± 2.0 mV); for the Co(II) reduction $E^{\circ\prime}$ = 1.212 V

Table IV. Cyclic Voltammetric and Spectroelectrochemical Results for Cobalt Complexes in OTTLE[a]

		cyclic voltammetry[b]	spectroelectrochemistry[c]	
complex	process	$E^{\circ\prime}$, V vs. NaSCE	$E^{\circ\prime}$, V vs. NaSCE	n
Co[(sal)$_2$en]	II → III	+0.040 (2)	+0.029 (407)	0.93
	II → I	−1.193 (6)	−1.198 (708)	1.03
Co[(sal)$_2$DAB)]	II → III	+0.085 (0)	+0.074 (383)	0.97
	II → I	−1.075 (0)	−1.055 (350)	0.98
Co[(sal)$_2$(3,4-DAEB)]	II → III	+0.070 (2)	+0.074 (385)	0.96
	II → I	−1.095 (2)	−1.090 (352)	1.01
Co[(sal)$_2$(2,3-DAN)]	II → III	+0.045 (3)	+0.054 (390)	0.98
	II → I	−1.067 (3)	−1.069 (336)	0.97
Co[(benac)$_2$en]	II → III	+0.099 (3)	+0.105 (435)	0.89
	II → I	−1.542 (5)[d]	*e*	*e*
Co[(naph)$_2$en]	II → III	+0.082 (2)	+0.064 (440)	0.92
	II → I	−1.201 (2)	−1.212 (425)	0.95
Co[(naph)$_2$DAB]	II → III	+0.049 (1)	*f*	*f*
	II → I	−1.108 (2)	*f*	*f*
Co[(naph)$_2$(3,4-DAEB)]	II → III	+0.078 (3)	+0.067 (400)	1.07
	II → I	−1.098 (3)	−1.093 (360)	0.90
Co[(naph)$_2$(2,3-DAN)]	II → III	+0.035 (2)	*f*	*f*
	II → I	+0.067 (4)	*f*	*f*

[a] Conditions: (complex) = (1.0–3.5) × 10^{-3} M; 0.5 M TEAP in DMF; 25 °C. The spectroelectrochemical results are considered to be the more thermodynamically meaningful—see text. [b] From Au OTTLE cyclic voltammetry at 2.0 mV/s; estimated standard deviation (mV) in parentheses. [c] From spectropotentiostatic method; analytical wavelength (nm) in parentheses. [d] From Hg–Au OTTLE cyclic voltammetry. [e] Anomalous behavior prevented analysis. [f] Low solubility prevented analysis.

Table V. Spectrophotometric Data for Cobalt Complexes from Spectroelectrochemical Experiments[a]

complex	Co(III) λ_{max}	Co(I) λ_{max}
Co[(sal)$_2$en]	380 (6900)	708 (21 800)
Co[(sal)$_2$DAB]	454 sh (14 000), 444 sh (14 200), 384 (18 400), 330 sh (27 300)	1200, 1081, 450 sh (12 000), 427 sh (14 400), 390 sh (20 700)
Co[(sal)$_2$(3,4-DAEB)]	455 sh (14 200), 440 br (14 200), 390 (18 600), 350 sh (24 100)	1175, 1078, 448 sh (9400), 428 sh (11 400), 390 sh (17 200)
Co[(sal)$_2$(2,3-DAN)]	462 sh (12 300), 415 (15 200)	1088, 975, 645 br (5500), 385 sh (25 900), 337 (37 600)
Co[(benac)$_2$en]	373 (12 800)	811, 545 br
Co[(naph)$_2$en]	417 (7900), 397 (8300)	765 (23 600), 610 br (8100), 470 br (5400)
Co[(naph)$_2$DAB][b]	516, 485, 415, 400	1200, 1125–1050 br, 488, 455, 375
Co[(naph)$_2$(3,4-DAEB)]	500 sh (14 000), 476 (16 700), 421 (17 200), 404 sh (15 300), 398 sh (15 100), 365 (19 800), 340 (20 100)	1188, 1075, 650 br (600), 485 sh (17 300), 462 (20 700), 373 (28 200)
Co[(naph)$_2$(2,3-DAN)][b]	436, 378, 340 sh	1150, 1096, 433 br, 390

[a] λ_{max} in nm; ϵ given in parentheses in M^{-1} cm^{-1}; sh = shoulder, br = broad; 0.5 M TEAP/DMF medium; ϵ not determined for near-IR bands. [b] Low solubility prevents determination of ϵ.

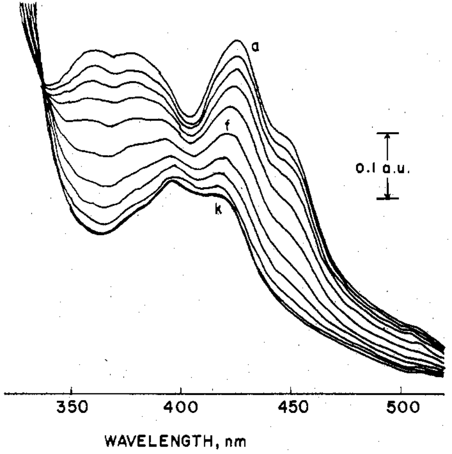

Figure 3. Spectra of Co[(naph)$_2$en], Co(II) → Co(III) process, in an optically transparent thin-layer electrode for a series of potentials. E_{app}: (a) −0.200, (b) −0.020, (c) +0.010, (d) +0.030, (e) +0.050, (f) +0.070, (g) +0.090, (h) +0.110, (i) +0.140, (j) +0.190, (k) +0.250 V vs. NaSCE.

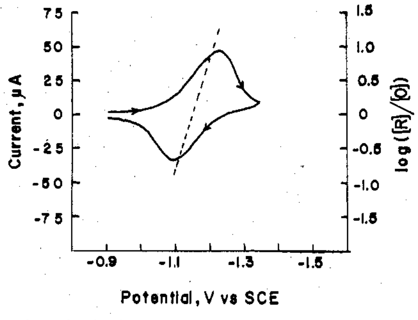

Figure 4. Left axis (—): thin-layer cyclic voltammogram of 1.25 mM Cu[(naph)$_2$en] in 0.5 M TEAP/DMF; scan rate 2 mV/s. Right axis (---): Nernstian plot of log ([R]/[O]) vs. E_{app} for the Cu(I)/Cu(II) couple.

and n = 1.02 electrons (slope = 58.2 ± 2.0 mV). The Nernstian reversibility of these two redox couples under these "equilibrium" experimental conditions is established by the linearity of the E_{app} vs. log ([R]/[O]) plots (correlation coefficient = 0.99 for both plots). This is to be compared with the above described quasi-reversible behavior under "kinetic" cyclic voltammetric conditions in bulk solution.

The above Nernstian behavior is typical of all the cobalt complexes investigated except for two of limited solubility and one of anomalous behavior. Table IV summarizes these results, and Table V lists spectrophotometric data for the fully oxidized and fully reduced cobalt complexes.

Copper Complexes. Results for copper complexes are generally similar to those for cobalt. Figure 4 shows a rep-

Table VI. Cyclic Voltammetric and Spectroelectrochemical Results for the Reduction of Copper(II) Complexes in OTTLE[a]

	cyclic voltammetry[b]	spectroelectrochemistry[c]		coulometry[d]
complex	$E°'$, V vs. NaSCE	$E°'$, V vs. NaSCE	n	n
Cu[(sal)$_2$en]	−1.150 (5)	*e*	*e*	1.01
Cu[(sal)$_2$DAB]	−1.081 (3)	*e*	*e*	0.97
Cu[(sal)$_2$(3,4-DAEB)]	−1.076 (1)	*e*	*e*	0.95
Cu[(sal)$_2$(2,3-DAN)]	−1.058 (1)	*e*	*e*	0.97
Cu[(benac)$_2$en]	−1.397 (13)[f]			
Cu[(acac)$_2$en]	−1.58[f]			
Cu[(naph)$_2$en]	−1.165 (4)	−1.152 (430)	0.98	
Cu[(naph)$_2$DAB]	−1.052 (2)	−1.040 (375)	0.99	
Cu[(naph)$_2$(3,4-DAEB)]	−1.054 (2)	−1.066 (375)	0.97	
Cu[(naph)$_2$(2,3-DAN)]	−1.037 (1)	−1.032 (378)	1.03	

[a] Conditions: (complex) = (1.0–2.5) × 10^{-3} M; 0.5 M TEAP in DMF; 25 °C. The spectroelectrochemical results are considered to be the more thermodynamically meaningful–see text. [b] From Au OTTLE cyclic voltammetry at 2.0 mV/s; estimated standard deviation (mV) in parentheses. [c] From spectropotentiostatic method; analytical wavelength (nm) in parentheses. [d] From controlled-potential coulometry (see text). [e] Anomalous behavior prevented analysis (see text). [f] Irreversible; E_p values listed.

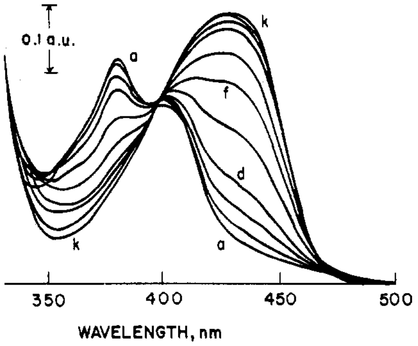

Figure 5. Spectra of Cu[(naph)$_2$en], Cu(II) → Cu(I) process, in an optically transparent thin-layer electrode for a series of potentials. E_{app}: (a) open circuit, (b) −1.080, (c) −1.100, (d) −1.130, (e) −1.150, (f) −1.170, (g) −1.190, (h) −1.220, (i) −1.250, (j) −1.300, (k) −1.350 V vs. NaSCE.

Table VII. Spectrophotometric Data for Electrogenerated Cu(I) Species[a]

complex	Cu(I) λ_{max}
Cu[(sal)$_2$en]	403 (13 100)
Cu[(sal)$_2$DAB]	385 (18 600)
Cu[(sal)$_2$(3,4-DAEB)]	436 sh (13 900), 390 (19 600)
Cu[(sal)$_2$(2,3-DAN)]	410 (22 900)
Cu[(benac)$_2$en][b]	352
Cu[(acac)$_2$en][b]	<300
Cu[(naph)$_2$en]	425 (16 100), 407 sh (15 500)
Cu[(naph)$_2$DAB]	460 sh (18 600), 433 br (21 300)
Cu[(naph)$_2$(3,4-DAEB)]	465 sh (22 700), 432 (27 000)
Cu[(naph)$_2$(2,3-DAN)]	480 sh (28 600), 442 br (33 700), 340 sh (31 600)

[a] See footnote *a*, Table V. [b] Irreversible couple–see Table VI.

resentative thin-layer cyclic voltammogram for Cu[(naph)$_2$en]. The only electrochemical behavior observed is a redox couple with $E°' = -1.165$ V and $\Delta E_p = 135$ mV. Quasi-reversibility is again indicated by the peak separation in bulk solution cyclic voltammetry. Repeated scans yield identical results. Thin-layer coulometry indicates a one-electron reduction and reoxidation.

Spectropotentiostatic measurements on Cu[(naph)$_2$en], Figure 5, indicate a one-electron redox process with $E°' = -1.152$ V. Nernstian reversibility under thin-layer conditions is again demonstrated by linearity of the E_{app} vs. log ([R]/[O]) plot, Figure 4 (correlation coefficient = 0.99). Table VI summarizes electrochemical data for the copper complexes, and Table VII gives spectrophotometric data for the Cu(I) species. The spectropotentiostatic data for the first four complexes of Table VI are not reliable due to a chemical process following the Cu(II) → Cu(I) electrochemical step; coulometric n values are given for these complexes. Two complexes, Cu[(benac)$_2$en] and Cu[(acac)$_2$en], give irreversible reductions at scan rates up to 3 V/s (bulk solution cyclic voltammetry). Values for $E°'$ and n are in agreement with literature values for those complexes which have been previously investigated.[19,22]

Discussion

Electrochemical Techniques. Thin-layer spectroelectrochemistry, utilizing the spectropotentiostatic technique, proved to be the most useful and meaningful of the experimental methods employed in this work. In these studies of cobalt and copper complexes, the spectropotentiostatic method allows simultaneous determination of (1) quantitative spectrophotometric parameters for both redox partners, (2) the $E°'$ value for the redox process, and (3) the n value associated with this process. Also, redox processes that are *quasi-reversible* under conditions of bulk solution cyclic voltammetry become *reversible* on the very slow time scale of OTTLE spectropotentiostatic experiment wherein each individual potential is maintained until equilibrium at that potential is reached. Thus, thermodynamically meaningful $E°'$ values can be obtained from the OTTLE technique, and the results of this study suggest that the OTTLE technique may be generally applicable to many of the redox systems that fall into the promiscuous category of "quasi-reversible." Also, because of the design of the OTTLE cell and the mechanics of the experiment, thin-layer spectroelectrochemistry provides a convenient method for obtaining the spectra of air-sensitive species such as Co(I). Exhaustive electrolysis within the OTTLE ensures that only the Co(I) species is present in the light path, and extraneous dioxygen can diffuse into the OTTLE only very slowly. With conventional methods it is very difficult to manipulate strongly reducing Co(I) solutions without suffering some extraneous oxidation.

Cobalt Complexes. While the range of $E°'$ values observed for the 10 Co(II)/Co(III) couples of Table IV is only 0.08 V, the corresponding range for the Co(I)/Co(II) couples is 0.49 V. This greater sensitivity of the Co(I)/Co(II) couple to the chemical structure of the equatorial ligand system is in agreement with observations[38,39] made on cobalt macrocyclic complexes. Busch[38] has noted that insensitivity of the Co(II)/Co(III) couple is probably dependent upon weak-field ligands being present in the axial coordination sites (so that the electron is removed from a predominantly d_{z^2} antibonding orbital of cobalt(II)), a condition which is met for the complexes of Table IV which contain solvent DMF as axial ligands. The metal–ligand π bonding which stabilizes the Co(I) oxidation state is reflected in the $E°'$ values of the Co(I)/Co(II) couple. In agreement with previous observations[38,40] on cobalt macrocyclic complexes, the data of Table IV show that increasing the number of aromatic rings

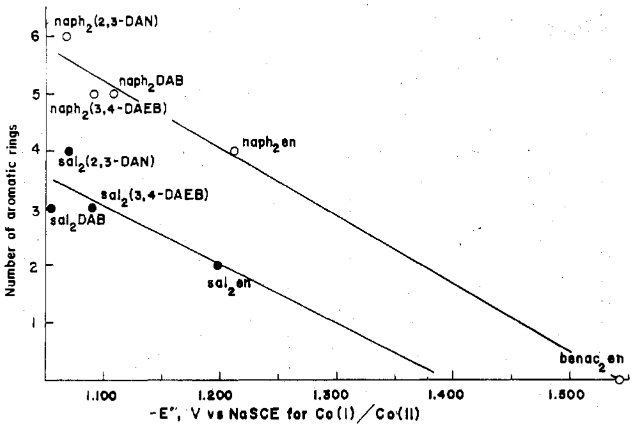

Figure 6. Plot of number of aromatic rings in the Schiff base ligands vs. $E^{\circ\prime}$ for the Co(I)/Co(II) couple.

or double bonds in the equatorial ligand facilitates reduction of cobalt(II) to cobalt(I). Figure 6 illustrates this general dependence of $E^{\circ\prime}$ on the number of aromatic rings, the data for the salicylaldehyde- and naphthaldehyde-based complexes showing an approximately parallel dependence. As a class, the naphthaldehyde-based complexes are more easily reduced than the salicylaldehyde-based complexes, and within each class the complex with the saturated backbone (ethylene) is the most difficult to reduce.

Spectra of the d^8 cobalt(I) complexes are dominated by an intense metal-to-ligand charge-transfer (MTLCT) band in the near-infrared region.[41,42] Within a related series of complexes, this band shifts to lower energy as it becomes more difficult to electrochemically reduce the cobalt(II) complex. E.g., Tables IV and V yield the following Co(I)/Co(II) $E^{\circ\prime}$ and Co(I) $\lambda_{\max}$ values (in V and nm) for the three complexes with an ethylenediimine bridge: −1.193, 708; −1.201, 765; −1.542, 811. While this relationship between $E^{\circ\prime}$ and $\lambda_{\max}$ is in the direction expected for a MTLCT band, i.e., the more difficult it is to reduce Co(II) to Co(I), the easier it is for Co(I) to transfer charge ("reduce") the ligand upon irradiation, the data are neither extensive nor accurate enough to warrant a detailed analysis.

Copper Complexes. Trends in the electrochemical behavior of the Cu(I)/Cu(II) couple are remarkably similar to those observed for the Co(I)/Co(II) couple. The sensitivity of $E^{\circ\prime}$ to equatorial ligand structure is demonstrated by the last four entries (those that do not exhibit anomalous or irreversible behavior) of Table VI; the Cu(I)/Cu(II) $E^{\circ\prime}$ range is 0.128 V while the comparable Co(I)/Co(II) $E^{\circ\prime}$ range is 0.134 V. Similarly, a plot of Cu(I)/Cu(II) $E^{\circ\prime}$ values vs. number of aromatic rings in the ligand (Figure 7) is very similar to the analogous cobalt plot (Figure 6). Thus, increasing the number of aromatic rings increases the stability of Cu(I), the naphthaldehyde-based complexes form a class that are more easily reduced than the salicylaldehyde-based complexes, and within each class the complex with the saturated backbone is the most difficult to reduce. These observations are in qualitative agreement with a previous report[43] that Cu(I) forms more stable complexes with macrocyclic ligands that contain a high degree of unsaturation.

Comparison of Co(II) and Cu(II) Reductions. In general, reduction of Cu(II) Schiff base complexes occurs more easily than reduction of the analogous Co(II) complexes. This is expected from the general chemistry of these elements and from previous observations[40] on macrocyclic complexes. Much more remarkable is the similar dependences of the Cu(I)/Cu(II) and Co(I)/Co(II) couples on equatorial ligand structure (with the common axial ligand DMF); this is illustrated in Figure 8 wherein $E^{\circ\prime}$ values for the two couples are plotted vs. each other. Except for the complexes derived from DAB, data for the salicylaldehyde-based complexes fall on a straight line of slope ca. 0.8, and data for the naphthaldehyde-based complexes fall on a parallel line. The DAB points are assumed to lie off the lines of Figure 8 because of experimental difficulties encountered in obtaining these specific data[32] (Tables IV and VI), although the possibility that there are unique interactions between the metal centers and the DAB-based ligands cannot be excluded (DAB is known[44] to be a noninnocent ligand). On a theoretical basis, the linear relationship between copper and cobalt couples as a function of equatorial ligand structure can be qualitatively understood since the two 3d electrons which differentiate d^8 Co(I) from d^{10} Cu(I) reside in the σ $d_{x^2-y^2}$ orbital—this orbital does not interact with the ligand π orbitals which stabilize Co(I) and Cu(I) by back-bonding. On an empirical basis, the linear relationships of Figure 8 strongly imply that the effects of varying equatorial ligand structure on $E^{\circ\prime}$ values are coherent and therefore at least predictable, even if not explicable, from one system to the next. This empirical observation should prove of value in "fine-tuning" $E^{\circ\prime}$ values of metal macrocyclic and Schiff base complexes used as models for biological redox components.

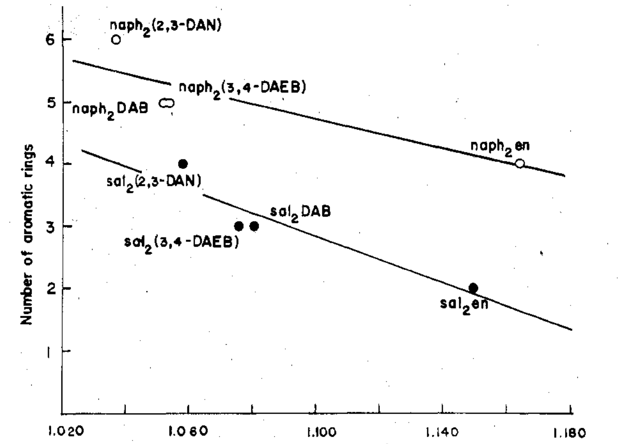

Figure 7. Plot of number of aromatic rings in the Schiff base ligands vs. $E^{\circ\prime}$ for the Cu(I)/Cu(II) couple.

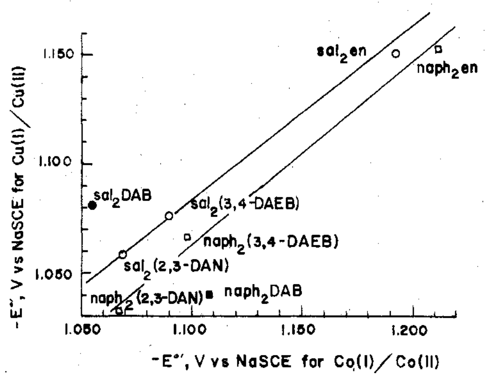

Figure 8. Plot of $E^{\circ\prime}$ for the Cu(I)/Cu(II) couple vs. $E^{\circ\prime}$ for the Co(I)/Co(II) couple. The ● and ■ points are not used in the correlation discussion (see text). Data are from this work.

Acknowledgment. This research was supported by National Science Foundation Grants CHE 77-04399 (W.R.H.) and CHE 76-19681 (E.D.). We thank the research group of W.R.H. for technical assistance and many helpful discussions.

Registry No. (sal)$_2$(3,4-DAEB), 70703-29-6; (sal)$_2$(2,3-DAN), 29506-34-1; (naph)$_2$(3,4-DAEB), 70714-15-7; (naph)$_2$(2,3-DAN), 70703-30-9; Co[(sal)$_2$(3,4-DAEB)], 70713-67-6; Co[(sal)$_2$(2,3-DAN)], 70749-41-6; Co[(naph)$_2$(3,4-DAEB)], 70713-68-7; Co[(naph)$_2$(2,3-DAN)], 70713-69-8; Cu[(sal)$_2$(3,4-DAEB)], 70749-42-7; Cu[(sal)$_2$(2,3-DAN)], 30172-33-9; Cu[(naph)$_2$(3,4-DAEB)], 70713-70-1; Cu[(naph)$_2$(2,3-DAN)], 70713-72-3; Co[(sal)$_2$en], 36870-54-9; Co[(sal)$_2$DAB], 39836-45-8; Co[(benac)$_2$en], 36802-28-5; Co[(naph)$_2$en], 33271-28-2; Co[(naph)$_2$DAB], 33271-29-3; [Cu[(sal)$_2$en], 34754-33-1; Cu[(sal)$_2$DAB], 42490-12-0; Cu[(benac)$_2$en], 15277-26-6; Cu[(acac)$_2$en], 36885-37-7; Cu[(naph)$_2$en], 36294-60-7; Cu[(naph)$_2$DAB], 20506-87-0; Co[(sal)$_2$en]$^+$, 66511-70-4; Co[(sal)$_2$en]$^-$, 26220-77-9; Co[(sal)$_2$DAB]$^+$, 70713-73-4; Co[(sal)$_2$DAB]$^-$, 56811-23-5; Co[(sal)$_2$(3,4-DAEB)]$^+$, 70713-74-5; Co[(sal)$_2$(3,4-DAEB)]$^-$, 70713-75-6; Co[(sal)$_2$(2,3-DAN)]$^+$, 70713-76-7; Co[(sal)$_2$(2,3-DAN)]$^-$, 70713-77-8; Co[(benac)$_2$en]$^+$, 70713-78-9; Co[(benac)$_2$en]$^-$, 70713-94-9; Co[(naph)$_2$en]$^+$, 70713-79-0; Co[(naph)$_2$en]$^-$, 70749-45-0; Co[(naph)$_2$DAB]$^+$, 70713-80-3; Co[(naph)$_2$DAB]$^-$, 70749-61-0; Co[(naph)$_2$(3,4-DAEB)]$^+$, 70713-81-4; Co[(naph)$_2$(3,4-DAEB)]$^-$, 70713-82-5; Co[(naph)$_2$(2,3-DAN)]$^+$, 70713-83-6; Co[(naph)$_2$(2,3-DAN)]$^-$, 70713-84-7; Cu[(sal)$_2$en]$^-$, 70749-46-1; Cu[(sal)$_2$DAB]$^-$, 70713-85-8; Cu[(sal)$_2$(3,4-DAEB)]$^-$, 70713-86-9; Cu[(sal)$_2$(2,3-DAN)]$^-$, 70713-87-0; Cu[(benac)$_2$en]$^-$, 70713-93-8; Cu[(acac)$_2$en]$^-$, 70713-92-7; Cu[(naph)$_2$en]$^-$, 70713-88-1; Cu[(naph)$_2$DAB]$^-$, 70713-89-2; Cu[(naph)$_2$(3,4-DAEB)]$^-$, 70713-90-5; Cu[(naph)$_2$(2,3-DAN)]$^-$, 70713-91-6.

References and Notes

(1) To whom correspondence should be addressed.
(2) S. J. Lippard, Ed., *Prog. Inorg. Chem.*, **18** (1973).
(3) R. P. Hanzlik, "Inorganic Aspects of Biological and Organic Chemistry", Academic Press, New York, 1976.
(4) E. Ochiai, "Bioinorganic Chemistry: An Introduction", Allyn and Bacon, Boston, Mass., 1977.
(5) A. W. Addison, W. R. Cullen, D. Dolphin, and B. R. James, "Biological Aspects of Inorganic Chemistry", Wiley, New York, 1977.
(6) R. Dessy, J. Dillard, and L. Taylor, Eds., *Adv. Chem. Ser.*, **No. 100** (1971).
(7) K. N. Raymond, Ed., *Adv. Chem. Ser.*, **No. 162** (1977).
(8) R. H. Abeles, ref 5, p 245.
(9) Reference 3, Chapter VIII.
(10) D. H. Busch et al., *Adv. Chem. Ser.*, **No. 100**, 44 (1971).
(11) G. N. Schrauzer, *Adv. Chem. Ser.*, **No. 100**, 1 (1971).
(12) R. G. Wilkins, *Adv. Chem. Ser.*, **No. 100**, 111 (1971).
(13) L. H. Vogt, Jr., H. M. Faigenbaum, and S. E. Wiberley, *Chem. Rev.*, **63**, 269 (1963).
(14) M. J. Carter, D. P. Rillema, and F. Basolo, *J. Am. Chem. Soc.*, **96**, 392 (1974).
(15) G. Costa, A. Puxeddu, and E. Reisenhofer, *J. Chem. Soc., Dalton Trans.*, 2034 (1973).
(16) D. F. Averill and R. F. Broman, *Inorg. Chem.*, **17**, 3389 (1978).
(17) M. Calvin and R. H. Bailes, *J. Am. Chem. Soc.*, **68**, 949 (1946).
(18) J. R. Urwin and B. O. West, *J. Chem. Soc.*, 4427 (1952).
(19) A. Bigotto, G. Costa, G. Mestroni, G. Pellizer, A. Puxeddu, E. Reisenhofer, L. Stefani, and G. Tauzher, *Inorg. Chim. Acta, Rev.*, **4**, 41 (1970).
(20) G. Costa, A. Puxeddu, and E. Reisenhofer, *J. Chem. Soc., Dalton Trans.*, 1519 (1972).
(21) G. Costa, J. Hanzlik, and A. Puxeddu, *J. Chem. Soc., Dalton Trans.*, 542 (1977).
(22) R. H. Holm and G. S. Patterson, *Bioinorg. Chem.*, **4**, 257 (1975).
(23) A. W. Addison, *Inorg. Nucl. Chem. Lett.*, **12**, 899 (1976).
(24) A. W. Addison and H. Yokoi, *Inorg. Chem.*, **16**, 1341 (1977).
(25) W. R. Heineman and T. Kuwana, *Acc. Chem. Res.*, **9**, 241 (1976).
(26) W. R. Heineman, *Anal. Chem.*, **50**, 390A (1978).
(27) W. R. Heineman and P. T. Kissinger, *Anal. Chem.*, **50**, 166R (1978).
(28) R. W. Murray, W. R. Heineman, and G. W. O'Dom, *Anal. Chem.*, **39**, 1666 (1967).
(29) T. P. DeAngelis and W. R. Heineman, *J. Chem. Educ.*, **53**, 594 (1976).
(30) A portion of this work has been previously reported: D. F. Rohrbach, E. Deutsch, and W. R. Heineman in "Characterization of Solutes in Nonaqueous Solvents", G. Mamantov, Ed., Plenum Press, New York, 1978.
(31) J. Halpern, L. G. Marzilli, and P. A. Marzilli, *J. Am. Chem. Soc.*, **93**, 1374 (1971).
(32) D. F. Rohrbach, Ph.D. Thesis, University of Cincinnati, 1977.
(33) T. P. DeAngelis, Ph.D. Thesis, University of Cincinnati, 1976.
(34) M. L. Meyer, T. P. DeAngelis, and W. R. Heineman, *Anal. Chem.*, **49**, 602 (1977).
(35) M. L. Meyer, M.S. Thesis, University of Cincinnati, 1976.
(36) G. W. Haupt, *J. Res. Natl. Bur. Stand.*, **48**, 2331 (1952).
(37) P. Kanatharan and M. S. Spritzer, *Anal. Lett.*, **6**, 421 (1973).
(38) A. M. Tait, F. V. Lovecchio, and D. H. Busch, *Inorg. Chem.*, **16**, 2206 (1977).
(39) D. P. Rillema and J. F. Endicott, *Inorg. Chem.*, **11**, 2361 (1972); D. P. Rillema, J. F. Endicott, and R. C. Patel, *J. Am. Chem. Soc.*, **94**, 394 (1972); D. P. Rillema and J. F. Endicott, *ibid.*, **94**, 8711 (1972).
(40) J. Vasilevskis and D. C. Olson, *Inorg. Chem.*, **10**, 1228 (1971).
(41) P. K. Das, H. A. O. Hill, J. M. Pratt, and R. J. P. Williams, *Biochim. Biophys. Acta*, **161**, 646 (1967).
(42) P. Day, G. Schregg, and R. J. P. Williams, *Biopolym. Symp.*, **1**, 271 (1964).
(43) D. C. Olson and J. Vasilevskis, *Inorg. Chem.*, **10**, 463 (1971).
(44) L. F. Warren, *Inorg. Chem.*, **16**, 2814 (1977).

Contribution from the Department of Chemistry, University of Pittsburgh, Pittsburgh, Pennsylvania 15260,
and The Pennsylvania State University, McKeesport, Pennsylvania 15132

Circular Dichroism Studies of Some Cobalt(III) Complexes Which Contain Phenyl-Substituted Ethylenediamine-*N*,*N*′-diacetate Analogues

GARY G. HAWN, CHRIS MARICONDI, and BODIE E. DOUGLAS*

Received December 8, 1978

The contributions from asymmetric nitrogens in cobalt(III) complexes to the rotational strengths can be significant depending upon the homogeneity of the chemical environment about the nitrogen atom. A complex has been prepared, [Co(*l*-sdda)en]$^+$ (*l*-sdda = *l*-stilbenediamine-*N*,*N*′-diacetate ion, en = ethylenediamine), which contains asymmetric nitrogens bonded to a hydrogen and a benzyl group, two substituents known to make opposite contributions to the rotational strength. The complex [Co(edda)(*l*-stien)]$^+$ (edda = ethylenediamine-*N*,*N*′-diacetate ion, *l*-stien = *l*-stilbenediamine) was prepared to estimate the contribution from the asymmetric carbons in *l*-stien. Some stereoselectivity was observed in the preparation of this complex. The carbon-13 NMR spectra for both complexes are reported, verifying that the complexes possess the s-cis geometry. Finally, several para-substituted *N*,*N*′-dibenzylethylenediamine-*N*,*N*′-diacetate (dbedda) cobalt(III) complexes have been prepared to study the electronic effects of substituents on asymmetric nitrogens.

Introduction

Circular dichroism (CD) studies of cobalt(III) complexes which contain edda, *N*,*N*′-dialkyl edda analogues, and *N*,*N*′-dibenzyl edda analogues coordinated in the s-cis geometry have been conducted extensively in the last decade.[1-6] Two important conclusions have been drawn. (1) The rotational strengths of the first ($^1T_{1g}$) CD band are insensitive to changes in the bidentate ligand occupying the non-edda sites.[4,6] This was attributed to the dominant influence of the rigid edda chelate. (2) It was found that the contribution of the asymmetric nitrogens (vicinal effect) to the rotational strength may be comparable in magnitude to that of the configurational effect.[1,2,6]

Maricondi and Maricondi[2] showed that asymmetric nitrogens in edda-type complexes may make opposite contributions to the rotational strength, depending upon whether the substituent on nitrogen is hydrogen or a benzyl group. They reached this conclusion by subtracting the CD curve of [Co(dmedda)en]$^+$ (dmedda = *N*,*N*′-dimethylethylenedi-

---

* To whom correspondence should be addressed at the University of Pittsburgh.